
A Novel Geometric Flow-Driven Approach for Quality Improvement of Segmented Tetrahedral Meshes

Juelin Leng¹, Yongjie Zhang², and Guoliang Xu¹ *

¹ LSEC, Institute of Computational Mathematics, Academy of Mathematics and System Sciences, Chinese Academy of Sciences, Beijing 100190, China
lengjl@lsec.cc.ac.cn, xuguo@lsec.cc.ac.cn

² Department of Mechanical Engineering, Carnegie Mellon University, USA
jessicaz@andrew.cmu.edu

Summary. This paper presents an efficient and novel geometric flow-driven method for mesh optimization of segmented tetrahedral meshes with non-manifold boundary surfaces. The presented method is composed of geometric optimization and topological transformation techniques, so that both location and topology of vertices are optimized. Non-manifold boundary can be divided into manifold surface patches having common boundary curves with each other. We adopt the averaged curvature flow to fair boundary curves with shape preserved, and the averaged mean curvature flow to fair surface patches with the property of volume-preserving. Meanwhile, boundary meshes are regularized by adjusting curve nodes and surface nodes along tangent directions. Locations of interior nodes are optimized by minimizing an energy functional which reflects the mesh quality. In addition, face-swapping and edge-removal operations are applied to eliminate poorly-shaped elements. Finally, we validate the presented method on several application examples, and the results demonstrate that mesh quality is improved significantly.

Key words: Segmented tetrahedral mesh, quality improvement, geometric flow-driven, optimization-based mesh smoothing, shape-preserving.

1 Introduction

Unstructured tetrahedral meshes for complex three dimensional domains have been recognized as indispensable tools in various application fields, including computer graphics, finite element simulations, and partial differential equations. Since mesh quality is an extremely critical factor influencing the stability, convergence, and accuracy of the numerical solution, tremendous efforts have been made to achieve better mesh quality. However, it is still a challenging problem to generate quality meshes for complicated structures with

*Corresponding author.

non-manifold boundaries. In finite element analysis, the research objects are often segmented into multiple regions with respect to different physical attributes, chemical attributes, or material properties. Thus, quality segmented meshes, with conforming non-manifold boundaries, are needed for partitioned regions. In this paper, we focus on quality improvement of segmented tetrahedral meshes with boundary surface smoothed and shape preserved.

The advancing front technique [2], octree methods [3, 17], and Voronoi Delaunay-based methods [5, 14] are well studied techniques in unstructured mesh generation. Several mesh generation methods [24, 26] for domains with segmented regions have been developed in recent years. Unfortunately, these techniques cannot avoid the existence of distorted elements efficiently. Therefore, a post processing step is necessary to improve the overall quality of the meshes produced by automatic mesh generators.

The existing methods for mesh improvement fall into three typical categories [7, 14]: vertex insertion, topological transformation, and geometric optimization (also called mesh smoothing). It is intuitive to eliminate poor elements by adding vertices into meshes. Hence, vertex insertion methods are powerful ways to improve mesh quality. However, adding vertices will increase the number of mesh elements, which is not we would like to see. In topological transformation, several operations are implemented to reconnect vertices such that a set of adjacent elements are replaced by another set of elements with higher quality. Operations like edge/face swapping [7] and edge/multi-face removal [13, 22] are usually local, easy to implement, and effective in removing poor elements. The effect for mesh quality improvement is also limited since reconnections are considered within small regions. To alleviate the limitation, a new reconnection way was proposed in [19] for relatively larger polyhedron composed of 20 to 40 tetrahedra. There are mainly two types of mesh smoothing methods, Laplacian smoothing and optimization-based smoothing. Laplacian smoothing [1] is simple and inexpensive, but it does not guarantee an improvement of the mesh in quality metrics and also results in degraded or inverted elements. Thus, various optimization-based methods were proposed. In these approaches, the objective function is based on a quality metric such as solid angle [21], dihedral angle [22], Jacobian matrix [9], or condition number [12]. In addition, Chen et al [15, 16] defined the interpolation error as the quality metric based on the concept of optimal Delaunay triangulation.

Surface smoothing is an important step of mesh improvement, since the generated meshes are often bumpy and irregular on boundary surfaces. During smoothing, surface features should be well preserved rather than be treated as noise and smoothed. Therefore, shape-preserving approaches were developed rapidly. Geometric flows [8] have the powerful ability to preserve features and reduce volume shrinkage. The surface diffusion flow which keeps the object volume invariant was used in [18, 25] to remove noise. Moreover, surface fitting and curvature information were applied to surface smoothing in [23].

In this paper, we present an efficient and novel geometric flow-driven method for mesh optimization of segmented tetrahedral meshes with non-

manifold surfaces. Vertices of the original meshes are classified into four types: fixed vertices, curve vertices, surface vertices and interior vertices. Different vertices are handled by different strategies. For curve vertices, the averaged curvature flow for shape preserving is used to fair curves, and vertices are also modified along the tangential direction to achieve equi-distribution on curves. The averaged mean curvature flow, with the property of volume-preserving, is selected to remove bumpiness of surfaces by moving surface vertices along the normal direction. Meanwhile, an optimization objective function is defined to regularize triangular surface meshes. Interior vertices are regularized by an optimization-based method, with the objective function reflecting mesh quality. These approaches can improve the overall mesh quality efficiently, but some poorly-shaped elements still exist, because some vertices have bad valence. Hence, supplement operations like face-swapping and edge-removal are joined into the mesh improvement process. Our experiment results demonstrate that the presented method improves mesh quality significantly and preserves surface boundary features efficiently.

The remainder of this paper is organized as follows: in section 2, we introduce the problem description and preparation work for mesh improvement; section 3 presents quality improvement algorithms and implementation details; several application examples are given in section 4 to demonstrate the effectiveness of the presented method; and conclusion is drawn in the end.

2 Problem Description and Preparation Work

This section gives the description of quality improvement problem for segmented tetrahedral meshes. Before performing the mesh optimization algorithms, some preparation work are needed. We classify all the vertices into four types and select proper quality metrics to measure the mesh quality.

2.1 Problem Description

Suppose we are given a tetrahedral mesh T in \mathbb{R}^3 , which is partitioned (segmented) into several volumetric components $\{T_i\}$. Fig. 1(a) shows a simple example of a segmented tetrahedral mesh with three components displayed by different colors. Our goal is to modify the mesh to regularize all the tetrahedra as much as possible. The given mesh is always bumpy and irregular on the boundary. Hence, we also aim to fair and regularize the boundary mesh with shape preserved.

For a given tetrahedral mesh, a position vector and a boundary indicator are given for each vertex, where the boundary indicator indicates if it lies on the boundary or not. Each tetrahedron is expressed by a list of its vertices in order. From the last vertex point of view, if the remaining three vertices are in the counterclockwise order, we say this tetrahedron is positive. If the ordering of a tetrahedron reverses this rule, then it is considered to be negative or inverted. In the given tetrahedral mesh, all tetrahedra are assumed to be positive. In addition, a component index is provided for each tetrahedron

indicating which component it belongs to. If a tetrahedron has a triangular face on the boundary, then two component indices are given as well, indicating which pair of components share this triangle.

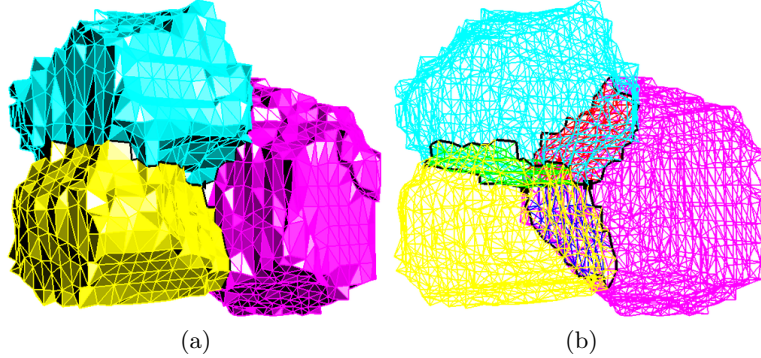


Fig. 1. (a) Tetrahedral mesh with three components; (b) the boundary mesh of (a).

2.2 Vertex Classification

Due to the complexity of non-manifold boundary, we classify the mesh vertices into four groups, such that different improvement strategies can be applied to each vertex group. Before vertex classification, we first introduce the concepts of boundary surface patches, boundary curves, and corner vertices.

Boundary surface patches: The common surface shared by any two components is referred to a boundary surface patch. Besides, the exterior boundary of each component is regarded as a boundary surface patch as well. As shown in Fig. 1(b), we use different colors to represent six boundary surface patches.

Boundary curves: The common curve shared by any two boundary surface patches is referred to a boundary curve, which is marked black in Fig. 1(b).

Corner vertices: The common vertex of any two boundary curves is referred to a corner vertex.

Then, we categorize the vertices into the following four groups:

Interior vertices: Interior vertices are vertices inside one volumetric component.

Surface vertices: Surface vertices are manifold vertices on boundary surface patches, which can move along the normal direction to remove noise, and move along the tangent direction to improve the aspect ratio of elements.

Curve vertices: Curve vertices are vertices located on boundary curves excluding end points. Curve vertices can only move along the tangent direction of the boundary curve during regularization.

Fixed vertices: Fixed vertices are end points of boundary curves and other non-manifold vertices, which are fixed during the mesh improvement process.

2.3 Quality Metrics of Tetrahedral Meshes

A number of quality metrics have been used to measure the quality of tetrahedral meshes, such as the longest-to-shortest edge length ratio [17], the minimum dihedral angle [22] or solid angle [21], and the element condition number [12]. Here, we choose the element aspect ratio introduced by Liu and Joe [4] to measure the tetrahedron quality,

$$Q = \frac{8 \cdot 3^{\frac{5}{2}} V}{(\sum_{j=1}^6 e_j^2)^{\frac{3}{2}}}, \tag{1}$$

where e_j are six edge lengths of one tetrahedron and V is the volume. If the oriented tetrahedron is positive, then the aspect ratio $Q \in [0, 1]$, and the quality gets better as Q is closer to 1.

Fig. 2 shows several examples of tetrahedra with poor quality. Tetrahedron (a) and (b) with one or two very short edges, can be recognized by all the above quality metrics. Four vertices of tetrahedra (c) and (d) are almost coplanar, but the ratios of the longest-to-shortest edge length are good. Tetrahedron (e) is slender but the minimum dihedral is away from 0 and π , so it cannot be detected by using the minimum dihedral angle as a quality metric. In contrast, the element aspect ratio Q can detect all the poor elements successfully.

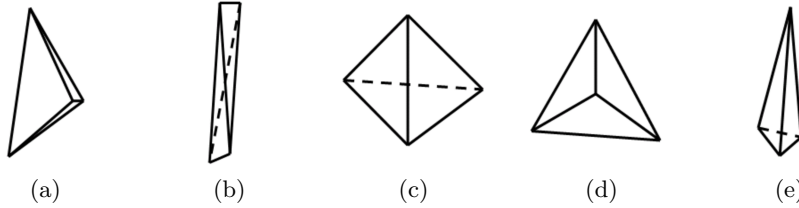


Fig. 2. Examples of poorly-shaped elements.

3 Quality Improvement Algorithm and Implementation

Our quality improvement algorithm for segmented tetrahedral meshes is composed of four steps:

1. Boundary curve fairing and regularization by adjusting curve vertices.
2. Boundary surface patch fairing and regularization by adjusting surface vertices.
3. Volume mesh regularization by relocating the interior vertices.
4. Topology improvement.

To fair a curve/surface mesh, we relocate the vertices such that the curve/surface is as smooth as possible. To regularize a curve/surface/volume

mesh, we relocate the mesh vertices so that each element of the mesh has an optimal shape in a certain sense.

The first three steps are geometric optimization for different groups of vertices, which are implemented and carried out iteratively. Then the topological transformations are used to optimize the connection of vertices. Geometric optimization and topological transformation are also performed iteratively, until the desirable result is achieved. In the following, we explain each step of the quality improvement algorithm in detail.

3.1 Curve Fairing by Averaged Curvature Flow

Let $[\mathbf{x}_0\mathbf{x}_1 \cdots \mathbf{x}_n]$ be a boundary curve of the mesh, which is actually a polygonal line. To fair this curve with shape preserved, we construct the following averaged curvature flow

$$\frac{d\mathbf{x}_i}{dt} = [\|\mathbf{h}_i(t)\| - h(t)] \mathbf{n}_i(t), \quad i = 1, \dots, n-1, \quad (2)$$

where

$$\mathbf{n}_i(t) = \frac{\mathbf{h}_i(t)}{\|\mathbf{h}_i(t)\|}, \quad \mathbf{h}_i(t) = \frac{\mathbf{t}_{i+1} - \mathbf{t}_i}{s_i}, \quad \mathbf{t}_i = \frac{\mathbf{x}_i - \mathbf{x}_{i-1}}{\|\mathbf{x}_i - \mathbf{x}_{i-1}\|}, \quad (3)$$

and

$$h(t) = \frac{\sum_{i=1}^{n-1} s_i \|\mathbf{h}_i\|}{\sum_{i=1}^{n-1} s_i}, \quad s_i = \frac{\|\mathbf{x}_i - \mathbf{x}_{i-1}\| + \|\mathbf{x}_i - \mathbf{x}_{i+1}\|}{2}. \quad (4)$$

The equation can be solved using the explicit Euler scheme

$$\mathbf{x}_i^{(k+1)} = \mathbf{x}_i^{(k)} + \tau [\|\mathbf{h}_i(t_k)\| - h(t_k)] \mathbf{n}_i(t_k), \quad i = 1, \dots, n-1, \quad (5)$$

where τ is a temporal step-size, $\mathbf{x}_i^{(0)} = \mathbf{x}_i$, and $\mathbf{x}_0^{(k)} = \mathbf{x}_0^{(k+1)} = \mathbf{x}_0$, $\mathbf{x}_n^{(k)} = \mathbf{x}_n^{(k+1)} = \mathbf{x}_n$. $\mathbf{h}_i(t_k)$, $h(t_k)$ and $\mathbf{n}_i(t_k)$ are defined in (3)–(4), taking $\mathbf{x}_i = \mathbf{x}_i^{(k)}$, $i = 0, \dots, n$.

Remark 1. To ensure that the vertex relocation will not result in inverted tetrahedra, we perform an explicit check. During each iteration step, if the relocation of vertices inverts any tetrahedron, we reduce the step-size by a predefined factor 0.618, until no inverted tetrahedron is produced. Similarly, this check will be used in the following algorithm.

3.2 Curve Regularization

Let $L = \sum_{i=1}^n \|x_i - x_{i-1}\|$. Then L is the total length of the polygonal line $[\mathbf{x}_0\mathbf{x}_1 \cdots \mathbf{x}_n]$. We intend to regularize the curve such that vertices are uniformly distributed. Therefore we construct the following energy functional

$$\mathcal{E}(\mathcal{C}) = \frac{1}{2} \sum_{i=1}^n (\|\mathbf{x}_i - \mathbf{x}_{i-1}\| - h)^2, \quad (6)$$

where $h = \frac{L}{n}$. At each free vertex \mathbf{x}_i of the curve, we vary \mathbf{x}_i as $\mathbf{x}_i \rightarrow \mathbf{x}_i + \epsilon_i \Phi_i$, $\Phi_i \in \mathbb{R}^3$, $i = 1, \dots, n-1$. Then $\mathcal{E}(\mathcal{C})$ can be denoted as $\mathcal{E}(\mathcal{C}, \epsilon_i)$ and

$$\begin{aligned} \left. \frac{\partial \mathcal{E}(\mathcal{C}, \epsilon_i)}{\partial \epsilon_i} \right|_{\epsilon_i=0} &= (\|\mathbf{x}_{i+1} - \mathbf{x}_i\| - h) \frac{\Phi_i^T (\mathbf{x}_i - \mathbf{x}_{i+1})}{\|\mathbf{x}_i - \mathbf{x}_{i+1}\|} \\ &\quad + (\|\mathbf{x}_i - \mathbf{x}_{i-1}\| - h) \frac{\Phi_i^T (\mathbf{x}_i - \mathbf{x}_{i-1})}{\|\mathbf{x}_i - \mathbf{x}_{i-1}\|}. \end{aligned}$$

Let \mathbf{e}_i be the unit tangential direction at \mathbf{x}_i , then we construct a set of L^2 -gradient flows as follows:

$$\frac{d\mathbf{x}_i}{dt} + (\|\mathbf{x}_{i+1} - \mathbf{x}_i\| - h) \frac{\mathbf{e}_i \mathbf{e}_i^T (\mathbf{x}_i - \mathbf{x}_{i+1})}{\|\mathbf{x}_i - \mathbf{x}_{i+1}\|} + (\|\mathbf{x}_i - \mathbf{x}_{i-1}\| - h) \frac{\mathbf{e}_i \mathbf{e}_i^T (\mathbf{x}_i - \mathbf{x}_{i-1})}{\|\mathbf{x}_i - \mathbf{x}_{i-1}\|} = \mathbf{0}, \quad (7)$$

$i = 1, \dots, n-1$. The discretization of (7) can be written as

$$\begin{aligned} \frac{\mathbf{x}_i^{(k+1)} - \mathbf{x}_i^{(k)}}{\tau} + (\|\mathbf{x}_{i+1}^{(k)} - \mathbf{x}_i^{(k)}\| - h) \frac{\mathbf{e}_i \mathbf{e}_i^T (\mathbf{x}_i^{(k)} - \mathbf{x}_{i+1}^{(k)})}{\|\mathbf{x}_i^{(k)} - \mathbf{x}_{i+1}^{(k)}\|} \\ + (\|\mathbf{x}_i^{(k)} - \mathbf{x}_{i-1}^{(k)}\| - h) \frac{\mathbf{e}_i \mathbf{e}_i^T (\mathbf{x}_i^{(k)} - \mathbf{x}_{i-1}^{(k)})}{\|\mathbf{x}_i^{(k)} - \mathbf{x}_{i-1}^{(k)}\|} = 0. \end{aligned} \quad (8)$$

The initial value is chosen as $\mathbf{x}_i^{(0)} = \mathbf{x}_i$. Each \mathbf{e}_i is obtained by computing the unit tangent direction of a fitting quadratic curve with respect to \mathbf{x}_{i-1} , \mathbf{x}_i and \mathbf{x}_{i+1} .

3.3 Surface Mesh Fairing by Averaged Mean Curvature Flow

To regularize a partitioned tetrahedral mesh, it is pre-requested that the volume of each component should be preserved. It is well known that for a compact (closed and finite) smooth surface, the averaged mean curvature flow is volume preserving. However, the problem here is different because the boundary surface consists of several surface patches with fixed boundary curves. Hence, the volume preserving property of the averaged mean curvature flow needs to be re-considered.

Let M_0 be a piece of compact orientable surface in \mathbb{R}^3 with boundary denoted as Γ . A curvature driven geometric evolution consists of finding a family $M = \{M(t) : t \geq 0\}$ of smooth orientable surfaces in \mathbb{R}^3 which evolve according to the flow equation

$$\frac{\partial \mathbf{x}}{\partial t} = V_n(\mathbf{x}) \mathbf{n}(\mathbf{x}), \quad M(0) = M_0, \quad \partial M(t) = \Gamma. \quad (9)$$

Here $\mathbf{x}(t)$ is a surface point on $M(t)$, $V_n(\mathbf{x})$ denotes the normal velocity of $M(t)$, and $\mathbf{n}(\mathbf{x})$ stands for the unit normal of the surface at $\mathbf{x}(t)$.

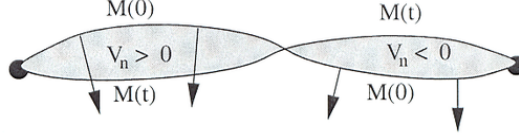


Fig. 3. The directional area between the curves $M(0)$ and $M(t)$. The area of the region with normal velocity $V_n > 0$ (or $V_n < 0$).

Theorem 1. Let $V(t)$ denote the (directional) volume of the region enclosed by $M(0)$ and $M(t)$ (see Fig. 3 for 2D curve case). Then we have

$$\frac{dV(t)}{dt} = \frac{1}{3} \int_{M(t)} V_n dA. \quad (10)$$

Proof. Let \mathcal{S} be a closed smooth surface and V be the volume enclosed by \mathcal{S} . Then we have (see [20]),

$$V = \frac{1}{3} \int_{\mathcal{S}} \mathbf{x}^T \mathbf{n} dA. \quad (11)$$

By taking derivative with respect to t , we have

$$\begin{aligned} \frac{dV(t)}{dt} &= \frac{1}{3} \frac{d}{dt} \left[\int_{M(t)} \mathbf{x}^T \mathbf{n} dA + \int_{M(0)} \mathbf{x}^T \mathbf{n} dA \right] \\ &= \frac{1}{3} \frac{d}{dt} \int_{M(t)} \mathbf{x}^T \mathbf{n} \sqrt{g} dudv \\ &= \frac{1}{3} \int_{M(t)} \left[\frac{d\mathbf{x}^T}{dt} \mathbf{n} \sqrt{g} + \mathbf{x}^T \frac{d(\mathbf{n} \sqrt{g})}{dt} \right] dudv. \end{aligned} \quad (12)$$

Since the flow is a normal motion of the surface without tangential movement, hence $\frac{d\mathbf{x}_u}{dt} = \frac{d\mathbf{x}_v}{dt} = \mathbf{0}$. We have $\frac{d(\mathbf{n} \sqrt{g})}{dt} = \mathbf{0}$. Substituting (9) into (12), we obtain

$$\frac{dV(t)}{dt} = \frac{1}{3} \int_{M(t)} V_n dA. \quad (13)$$

□

In (9), if we take $V_n = H(t) - h(t)$, where $h(t) = \int_{M(t)} H dA / \int_{M(t)} dA$, then we have the **Averaged Mean Curvature Flow** [10] (AMCF)

$$\frac{\partial \mathbf{x}}{\partial t} = [H(\mathbf{x}) - h(t)] \mathbf{n}(\mathbf{x}), \quad M(0) = M_0, \quad \partial M(t) = \Gamma. \quad (14)$$

The existence proof of the global solution to this flow can be found in Escher and Simonett's paper [6]. It follows from (10) that

$$\frac{dV(t)}{dt} = \frac{1}{3} \left(\int_{M(t)} H dA - h(t) \int_{M(t)} dA \right) = 0.$$

Hence the averaged mean curvature flow is volume preserving, and its steady solution depends upon the initial surface.

Let M be a triangular surface patch and $\{\mathbf{x}_i\}_{i=1}^N$ be its free vertex set. For a vertex \mathbf{x}_i with valence n , $N(i) = \{i_1, i_2, \dots, i_n\}$ denotes the index set of one-ring neighbors of \mathbf{x}_i . Equation (14) is solved for the triangular mesh M using an explicit discretization method, where the discrete approximation of the mean curvature vector, mean curvature and surface normal are required. These approximations can be found in [8, 20]. Moreover, to compute $h(t)$, the integration $\int_{M(t)} H dA$ can be discretized as $\sum_{i=1}^N [H(\mathbf{x}_i) A_M(\mathbf{x}_i)]$, where $A_M(\mathbf{x}_i)$, as shown in Fig. 4, denotes the area represented by \mathbf{x}_i .

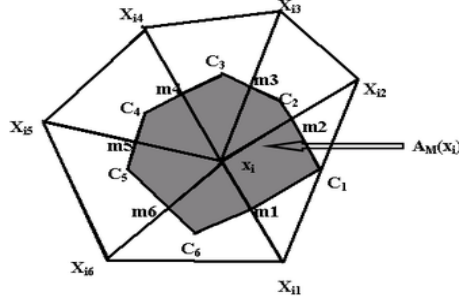


Fig. 4. Area represented by \mathbf{x}_i . $\{\mathbf{m}_j\}_{j=1}^6$ are midpoints of edges $[\mathbf{x}_i \mathbf{x}_{i_j}]$. \mathbf{c}_j is the circumcenter point for the triangle $[\mathbf{x}_{i_j} \mathbf{x}_{i_{j+1}} \mathbf{x}_i]$ if the triangle is non-obtuse; if the triangle is obtuse, \mathbf{c}_j is chosen to be the midpoint of the longest edge.

3.4 Surface Mesh Regularization

Suppose \mathcal{S} is a piece of triangular surface patch. We intend to regularize it with fixed boundary. Let m be the triangle number of \mathcal{S} , and A be the total area of all the triangles. Let $h = \frac{2}{3^{\frac{1}{4}}} \left(\frac{A}{m}\right)^{\frac{1}{2}}$. To make vertices equally distributed, we define

$$\mathcal{E}(\mathcal{S}) = \frac{1}{2} \sum_{i=1}^N \sum_{j \in N(i)} (\|\mathbf{x}_j - \mathbf{x}_i\| - h)^2. \quad (15)$$

At each free vertex \mathbf{x}_i , we vary \mathbf{x}_i as $\mathbf{x}_i \rightarrow \mathbf{x}_i + \epsilon_i \Phi_i$, where $\Phi_i \in \mathbb{R}^3$, $i = 1, \dots, N$. Then $\mathcal{E}(\mathcal{S})$ can be denoted as $\mathcal{E}(\mathcal{S}, \epsilon_i)$, and

$$\left. \frac{\partial \mathcal{E}(\mathcal{S}, \epsilon_i)}{\partial \epsilon_i} \right|_{\epsilon_i=0} = \sum_{j \in N(i)} (\|\mathbf{x}_j - \mathbf{x}_i\| - h) \frac{\Phi_i^T (\mathbf{x}_i - \mathbf{x}_j)}{\|\mathbf{x}_i - \mathbf{x}_j\|}.$$

Let $\mathbf{e}_i^{(1)}$ and $\mathbf{e}_i^{(2)}$ be two unit orthogonal tangential directions at \mathbf{x}_i . Then we construct two sets of L^2 -gradient flows as follows:

$$\frac{d\mathbf{x}_i}{dt} + \sum_{j \in N(i)} (\|\mathbf{x}_j - \mathbf{x}_i\| - h) \frac{\mathbf{e}_i^{(l)} (\mathbf{e}_i^{(l)})^T (\mathbf{x}_i - \mathbf{x}_j)}{\|\mathbf{x}_i - \mathbf{x}_j\|} = \mathbf{0}, \quad i = 1, \dots, N, \quad (16)$$

where $l = 1, 2$. Equation (16) is solved iteratively by an explicit Euler scheme for the unknown \mathbf{x}_i , $i = 1, \dots, N$. Tangential directions $\mathbf{e}_i^{(1)}$ and $\mathbf{e}_i^{(2)}$ can be computed from the limit surface of Loop's subdivision [11] or the quadratic fitting surface [20]. The discretization of (16) can be written as

$$\frac{\mathbf{x}_i^{(k+1)} - \mathbf{x}_i^{(k)}}{\tau} + \sum_{j \in N(i)} (\|\mathbf{x}_j^{(k)} - \mathbf{x}_i^{(k)}\| - h) \frac{\mathbf{e}_i^{(l)} (\mathbf{e}_i^{(l)})^T (\mathbf{x}_i^{(k)} - \mathbf{x}_j^{(k)})}{\|\mathbf{x}_i^{(k)} - \mathbf{x}_j^{(k)}\|} = 0,$$

with $i = 1, \dots, N$, and $l = 1, 2$. The initial value is chosen as $\mathbf{x}_i^{(0)} = \mathbf{x}_i$. $\mathbf{e}_i^{(1)}$ and $\mathbf{e}_i^{(2)}$ are computed using the data at step k .

Remark 2. In the energy functional (15), h is defined as a global constant with respect to the average area of all triangles. If the mesh is adaptive to various density of distribution, then the local h_i can be used for each free vertex \mathbf{x}_i , and the energy functional is replaced by $\mathcal{E}(\mathcal{S}) = \frac{1}{2} \sum_{i=1}^N \sum_{j \in N(i)} (\|\mathbf{x}_j - \mathbf{x}_i\| - h_i)^2$. h_i can be chosen as $\frac{2}{3^{1/4}} \cdot A_i$, where A_i is the average area of triangles surrounding \mathbf{x}_i . Similarly, in the curve regularization energy functional (6), h can be replaced by a local h_i for adaptive meshes as well.

In addition, both the global h and the local h_i are updated during the iteration process of curve regularization and surface regularization.

3.5 Volume Mesh Regularization

Let M be a tetrahedral mesh for one component, and $\{\mathbf{x}_i\}_{i=1}^N$ be its interior vertex set. For a vertex \mathbf{x}_i with tetrahedron valence n , let $N(i) = \{i_1, i_2, \dots, i_n\}$ be the index set of its one-ring tetrahedron neighbors.

Let \mathcal{T} be the set of all tetrahedra in M . Define the energy functional as

$$\mathcal{E}(M) = \mathcal{E}(\mathbf{x}_1, \dots, \mathbf{x}_N) = \frac{1}{2} \sum_{\tau \in \mathcal{T}} (Q_\tau - 1)^2, \quad (17)$$

where $Q_\tau = \frac{(\sum_{j=1}^6 e_{\tau,j}^2)^{3/2}}{8 \cdot 3^{3/2} V_\tau}$ is a quality metric, V_τ is the volume of tetrahedron τ , and $e_{\tau,j}$ ($j = 1, \dots, 6$) are six edge lengths of τ . Note that Q_τ^{-1} is just the quality metric given in section 2.3, and $Q_\tau = 1$ if and only if τ is a regular tetrahedron. Hence, the overall mesh quality is improved as the energy functional $\mathcal{E}(M)$ reduces. At each interior vertex \mathbf{x}_i , we vary \mathbf{x}_i as $\mathbf{x}_i \rightarrow \mathbf{x}_i + \epsilon_i \Phi_i$, where $\Phi_i \in \mathbb{R}^3$, $i = 1, \dots, N$. Then

$$\left. \frac{\partial \mathcal{E}(M, \epsilon_i)}{\partial \epsilon_i} \right|_{\epsilon_i=0} = \left. \frac{\partial \mathcal{E}(\mathbf{x}_1, \dots, \mathbf{x}_N, \epsilon_i)}{\partial \epsilon_i} \right|_{\epsilon_i=0} = \sum_{\tau \in N(i)} (Q_\tau(\epsilon_i) - 1) \left. \frac{\partial Q_\tau(\epsilon_i)}{\partial \epsilon_i} \right|_{\epsilon_i=0},$$

where

$$\frac{\partial Q_\tau(\epsilon_i)}{\partial \epsilon_i} \Big|_{\epsilon_i=0} = \frac{3(\sum_{j=1}^6 e_{\tau,j}^2)^{\frac{1}{2}} \sum_{k=1}^3 \Phi_i^T(\mathbf{x}_i - \mathbf{x}_{\tau,k})}{8 \cdot 3^{\frac{5}{2}} V_\tau} - \frac{(\sum_{j=1}^6 e_{\tau,j}^2)^{\frac{3}{2}} \frac{\partial V_\tau(\epsilon_i)}{\partial \epsilon_i} \Big|_{\epsilon_i=0}}{8 \cdot 3^{\frac{5}{2}} V_\tau^2}.$$

Here, τ is an adjacent tetrahedron of \mathbf{x}_i , $\mathbf{x}_{\tau,k}$ ($k = 1, 2, 3$) are the three other vertices of τ besides \mathbf{x}_i .

Suppose $\mathbf{x}_i, \mathbf{x}_{\tau,1}, \mathbf{x}_{\tau,2}$ and $\mathbf{x}_{\tau,3}$ are in the positive order, so that

$$\frac{1}{6} \begin{vmatrix} 1 & x_i & y_i & z_i \\ 1 & x_{\tau,1} & y_{\tau,1} & z_{\tau,1} \\ 1 & x_{\tau,2} & y_{\tau,2} & z_{\tau,2} \\ 1 & x_{\tau,3} & y_{\tau,3} & z_{\tau,3} \end{vmatrix} = V_\tau,$$

where $\mathbf{x}_i = (x_i, y_i, z_i)^T$, $\mathbf{x}_{\tau,k} = (x_{\tau,k}, y_{\tau,k}, z_{\tau,k})^T$, $k = 1, 2, 3$. Then

$$\begin{aligned} \frac{\partial V_\tau(\epsilon_i)}{\partial \epsilon_i} \Big|_{\epsilon_i=0} &= -\frac{1}{6} \Phi_i^T \left(\begin{vmatrix} 1 & y_{\tau,1} & z_{\tau,1} \\ 1 & y_{\tau,2} & z_{\tau,2} \\ 1 & y_{\tau,3} & z_{\tau,3} \end{vmatrix}, \begin{vmatrix} 1 & z_{\tau,1} & x_{\tau,1} \\ 1 & z_{\tau,2} & x_{\tau,2} \\ 1 & z_{\tau,3} & x_{\tau,3} \end{vmatrix}, \begin{vmatrix} 1 & x_{\tau,1} & y_{\tau,1} \\ 1 & x_{\tau,2} & y_{\tau,2} \\ 1 & x_{\tau,3} & y_{\tau,3} \end{vmatrix} \right)^T \\ &\triangleq -\frac{1}{6} \Phi_i^T \Psi_{\tau,i}. \end{aligned}$$

Therefore,

$$\begin{aligned} &\frac{\partial \mathcal{E}(M, \epsilon_i)}{\partial \epsilon_i} \Big|_{\epsilon_i=0} \\ &= \sum_{\tau \in N(i)} (Q_\tau - 1) \Phi_i^T \left(\frac{3(\sum_{j=1}^6 e_{\tau,j}^2)^{\frac{1}{2}} \sum_{k=1}^3 (\mathbf{x}_i - \mathbf{x}_{\tau,k})}{8 \cdot 3^{\frac{5}{2}} V_\tau} + \frac{(\sum_{j=1}^6 e_{\tau,j}^2)^{\frac{3}{2}} \Psi_{\tau,i}}{48 \cdot 3^{\frac{5}{2}} V_\tau^2} \right) \\ &\triangleq \Phi_i^T \mathbf{d}_i, \end{aligned}$$

where \mathbf{d}_i is the gradient direction of $\mathcal{E}(M)$ with respect to \mathbf{x}_i . Then, we get the following discrete scheme:

$$\mathbf{x}_i^{(k+1)} = \mathbf{x}_i^{(k)} - \alpha_k \mathbf{d}_i^{(k)}.$$

Here, α_k is the step size in the gradient direction $\mathbf{d}_i^{(k)}$, which is properly selected such that the energy functional decreases and the worst quality among neighboring tetrahedra of \mathbf{x}_i is also improved.

3.6 Topological Transformation

Most experiments show that, even after geometric optimization, some less-ideal elements still remain in the mesh. Thus, reconnection for mesh vertices should be considered. Face swapping, as the most popular topological operation, is used in our method to further improve the tetrahedral mesh. Basic operations for face swapping are shown in Fig. 5. These operations are simple, but it is critical to choose a proper algorithm.

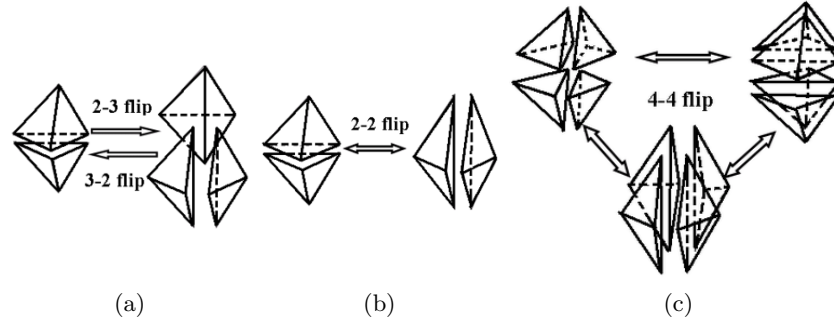


Fig. 5. Face swapping operations. (a) 2-3 and 3-2 flip; (b) 2-2 flip; (c) 4-4 flip.

Algorithm 1 presents our face swapping scheme for improving segmented tetrahedral mesh. Here, if the boundary is not destroyed and no inverted tetrahedron is produced, we say the operation is legal.

Algorithm 1 *Face swapping*

1. Compute the quality metric Q for all tetrahedra in the segmented mesh.
2. For each tetrahedron τ with $Q < \varepsilon$, where $\varepsilon \in (0, 1)$ is a given threshold, perform the following steps to find the optimal operation to improve the quality.
 - a. Set $f_i = -1.0, i = 1, \dots, 4$, and $e_i = -1.0, i = 1, \dots, 6$.
 - b. Check each face of the tetrahedron. If the 2-3 flip operation is legal for removing face i , then set f_i as the worst quality of the three new tetrahedra.
 - c. Check each edge of the tetrahedron.
 - If the valence of edge i is 3 and the 3-2 flip is legal, then set e_i as the worst quality of the two new tetrahedra.
 - If the edge is valence 4 and the 4-4 flip is legal, then set e_i as the worst quality if the operation performs.
 - If the edge with valence 2 is on an exterior boundary and the 2-2 flip is legal, then set e_i as the worst quality if the 2-2 flip performs.
 - d. If

$$\max\{\max_{i=1,\dots,4}\{f_i\}, \max_{i=1,\dots,6}\{e_i\}\} > Q,$$

perform the corresponding operation such that the worst quality reaches the maximum, and then update the quality Q of all the new tetrahedra.

3. Go back to step 1 until no operation can be performed or reach the given loop steps.

It is well known that edge swapping is a simple and efficient way to eliminate sliver triangles for triangular meshes. For tetrahedral meshes, we use edge removal operation [13] to swap boundary edges. Fig. 6 shows the process of removing boundary edge $[AB]$. The gray area is an interior boundary. After removing boundary edge $[AB]$, vertices C and D are connected to generate

two new boundary triangles. The next step is to find an optimal triangulation for the two polygons that maximize the quality of the worst tetrahedron. The edge removal operation is implemented by performing a sequence of 2-3 flips followed by a single 4-4 flip. For the exterior boundary edge removal, the last 4-4 flip in the interior case is replaced by a 2-2 flip.

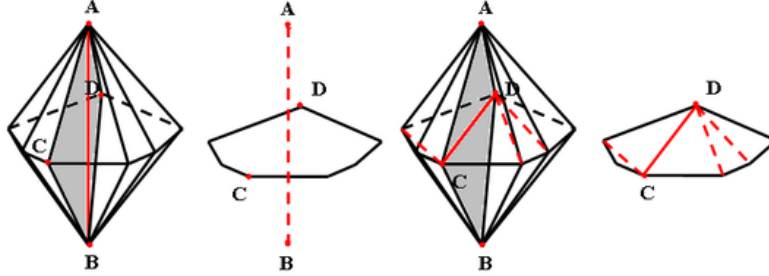


Fig. 6. An edge removal transformation.

4 Application Examples

In this section, we present several examples to show the efficiency of our new method. The input segmented meshes were generated by an octree-based iso-contouring method in [26].

4.1 Titanium Alloy with 52 Grains

The first example is a representative volume element of titanium alloy with 52 grains. The original tetrahedral mesh shown in Fig. 7(a) consists of 512,191 nodes and 3,000,564 tetrahedra. There are 3,678 elements with the quality value Q below 0.2, and the lowest value is 0.0002. Since the outline of the mesh is a cube, we treat the eight corners as fixed vertices, and treat vertices on the cube edges as curve points which can only move along the edge.

We improve the given mesh using the presented method and get the improved mesh displayed in Fig. 7(b), with each color representing a different grain. It is clear that planar boundary curves are smoothed and vertices are regularly distributed on curves. Moreover, sliver triangles near boundary curves in Fig. 7(a) are eliminated. Fig. 8 shows the improvement of interior boundary surface patches. Compared to the original mesh, both smoothness and regularity of the improved mesh are desirable. In addition, meshes of some internal grains are displayed in Fig. 9.

The mesh quality statistics before and after improvement are compared in Table 1, which shows a remarkable improvement of mesh quality using our method. The minimum quality value increases to 0.1346, and the average quality increases from 0.8721 to 0.8909. The mesh is overall optimized with

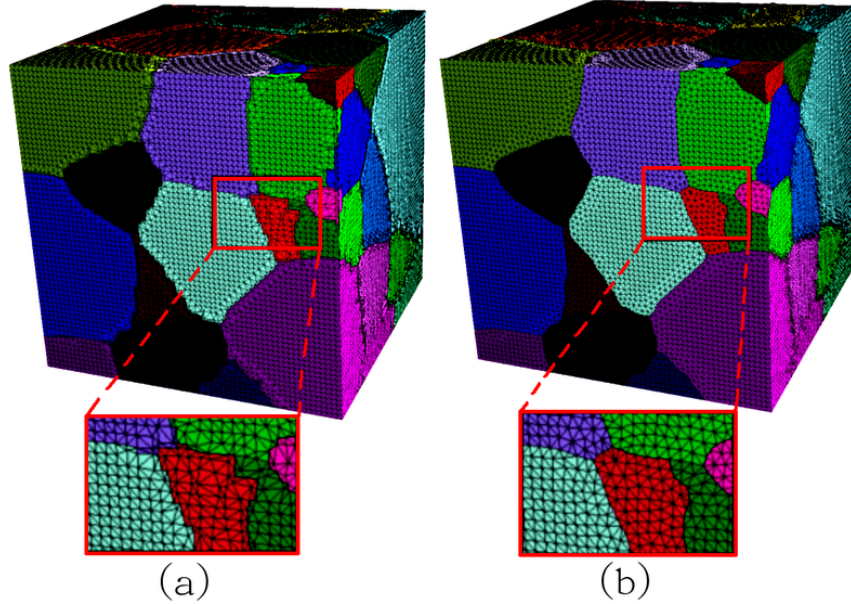


Fig. 7. (a) The original tetrahedral mesh; (b) the improved tetrahedral mesh.

good elements increased and poor elements reduced. Furthermore, six dihedral angles for all tetrahedra are calculated to measure the mesh quality, and the histogram of dihedral angles is plotted in Fig. 10 (Left). The black line denotes the original mesh with dihedral angles ranging from 0.009° to 179.98° , while the red line denotes the improved mesh with dihedral angles ranging from 5.83° to 153.43° . The red line has a gap near 10° with the percentage value equals to zero. The original mesh is generated by an octree-based method which has structured interior elements, that explains why two peaks appear in the chart.

Table 1. Quality comparison

Quality value	min	max	average	0-0.2	0.2-0.4	0.4-0.6	0.6-0.8	0.8-1.0
Original mesh	0.0002	0.9994	0.8721	3,678	36,190	128,830	284,705	2,547,161
Improved mesh	0.1346	0.9998	0.8909	7	835	26,305	381,840	2,591,614

4.2 Brain Model with 41 Components

The fairing and regularization methods for boundary curves and surfaces introduced in section 3 can be used to optimize triangular meshes as well. Here, we give an example for improving triangular boundary meshes of a brain model. The brain model is made up of 41 components, and the original tri-

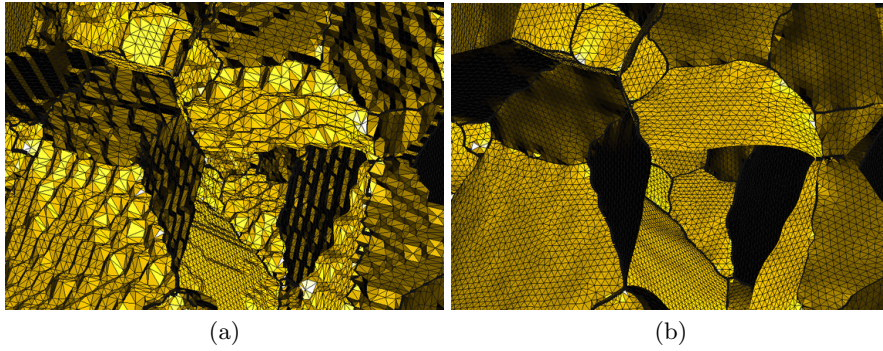


Fig. 8. Internal structure of the boundary mesh. (a) The original boundary mesh; (b) the smoothed boundary mesh.

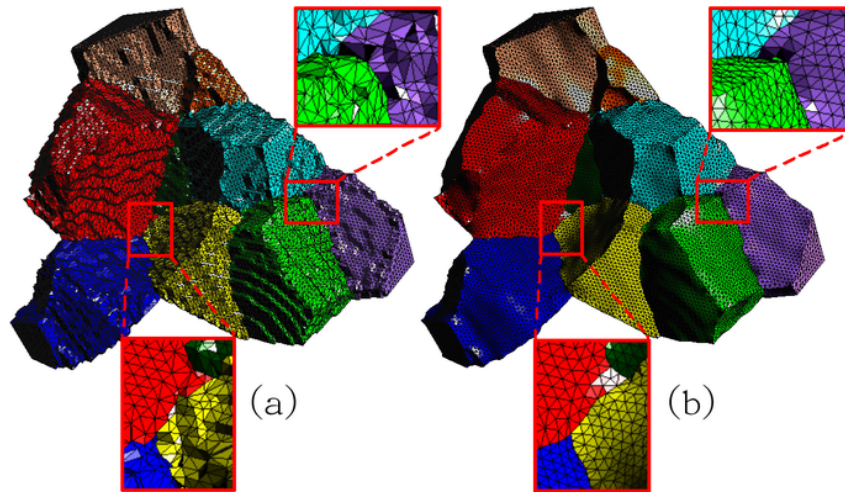


Fig. 9. Meshes of internal grains. (a) The original mesh; (b) the improved mesh.

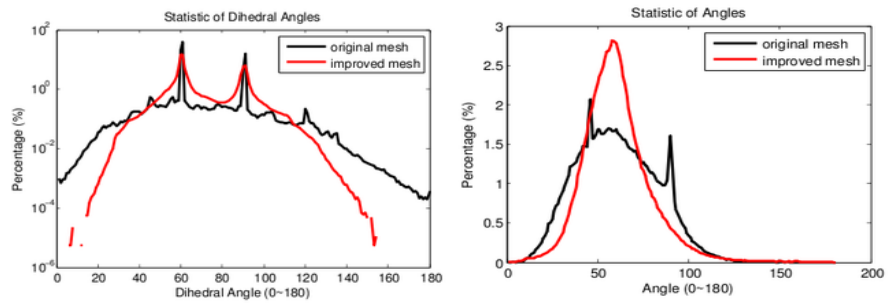


Fig. 10. Left: Dihedral angle statistics of the tetrahedral mesh in Fig. 7 (52-grain titanium alloy). Right: Angle statistics of the triangular mesh in Fig. 11 (brain).

angular mesh consists of 97,295 nodes and 211,222 triangles. We apply our algorithms to optimize the mesh.

Fig. 11(a) and (b) show the exterior boundary meshes for the original mesh and the improved mesh, respectively. Surface patches belong to different components are represented with different colors. It can be seen that, surface noise is removed successfully and triangles are much more regular. Fig. 12 shows the improvement performance on interior surface patches. The histogram of mesh angles is plotted in Fig. 10 (Right), with the black line standing for the original mesh and the red line standing for the improved mesh. After improvement, angles are away from 0° and 180° , with its density distribution close to a normal distribution.

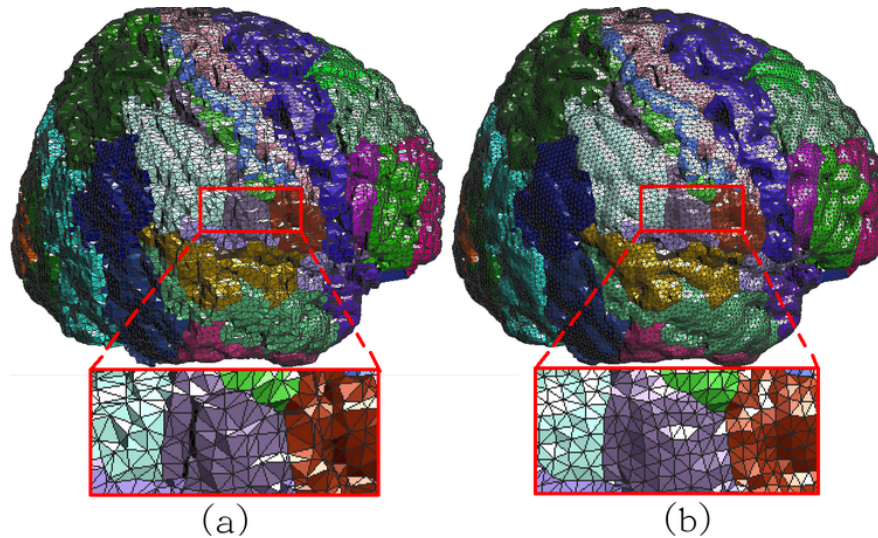


Fig. 11. (a) The original triangular mesh; (b) the improved triangular mesh.

5 Conclusion

We have presented a novel geometric flow-driven method for quality improvement of segmented tetrahedral meshes, with volume-preserving for each component. At first, mesh vertices are classified into four groups, and each group of vertices is relocated by various geometric optimization strategies. Moreover, face-swapping and edge-removal operations are applied to eliminate poorly-shaped elements by changing the topology of vertices. Finally, we validate the presented method on several examples. Experiment results indicate that our method is capable of significantly improving the quality of segmented tetrahedral meshes and efficiently preserving boundary features.

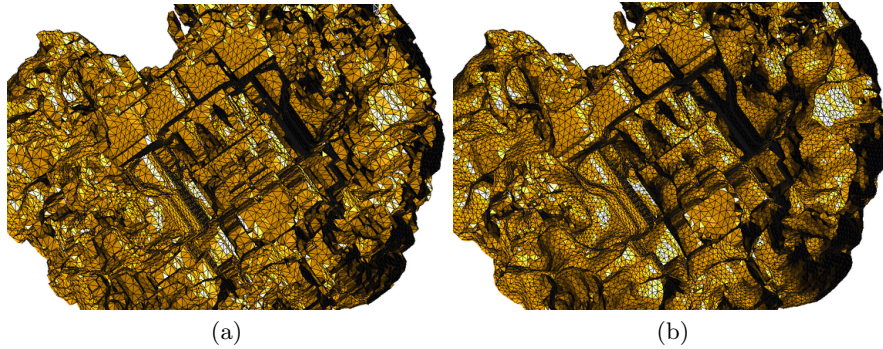


Fig. 12. Cross section of brain. (a) The original mesh; (b) the smoothed mesh.

Acknowledgement. Juelin Leng and Guoliang Xu were supported in part by NSFC under the grant 60773165, NSFC key project under the grant 10990013 and Funds for Creative Research Groups of China (grant No. 11021101). Yongjie Zhang was supported in part by a NSF/DOD-MRSEC seed grant. The authors are grateful to Jin Qian for preparing the tetrahedral mesh data.

References

1. Field D.(1988) Laplacian Smoothing and Delaunay Triangulation. *Communications in Applied Numerical Methods*, 4: 709-712.
2. Lohner R, Parikh P.(1988) Generation of Three-dimensional Unstructured Grids by the Advancing-front Method. *International Journal for Numerical Methods in Fluids*, 8: 1135-1149.
3. Shephard M S, Georges M K.(1991) Automatic Three-dimensional Mesh Generation Technique by the Finite Element Octree Technique. *International Journal for Numerical Methods in Engineering*, 32: 709-749.
4. Liu A, Joe B.(1994) Relationship Between Tetrahedron Quality Measures. *BIT*, 1994; 34: 268-287.
5. Borouchaki H, Lo S H.(1995) Fast Delaunay Triangulation in Three Dimensions. *Computer Methods in Applied Mechanics and Engineering*, 128: 153-167.
6. Escher J, Simonett G.(1998) The Volume Preserving Mean Curvature Flow Near Spheres. *Proceedings of the American Mathematical Society*, 126(9): 2789-2796.
7. Freitag L S, Ollivier-Gooch C.(1998) Tetrahedral Mesh Improvement Using Face Swapping and Smoothing. *International Journal for Numerical Methods in Engineering*, 40(21): 3979-4002.
8. Desbrun M, Meyer M, Schröder P, Barr A H.(1999) Implicit Fairing of Irregular Meshes Using Diffusion and Curvature Flow. *SIGGRAPH99*, 317-324, Los Angeles, USA.
9. Knupp P M.(2000) A Framework for Volume Mesh Optimization and the Condition Number of the Jacobian Matrix. *International Journal For Numerical Methods In Engineering*, 48(8): 1165-1185.

10. Sapiro G.(2001) Geometric Partial Differential Equations and Image Analysis. Cambridge, University Press.
11. Bajaj C, Xu G, Warren J.(2002) Acoustics Scattering on Arbitrary Manifold Surfaces. In Proceedings of Geometric Modeling and Processing, Theory and Application, Japan, 73-82.
12. Freitag LA, Knupp PM.(2002) Tetrahedral Mesh Improvement via Optimization of the Element Condition Number. International Journal for Numerical Methods in Engineering, 53: 1377-1391.
13. Shewchuk JR.(2002) Two Discrete Optimization Algorithms for the Topological Improvement of Tetrahedral Meshes. Unpublished manuscript.
14. Du Q, Wang D.(2003) Tetrahedral Mesh Generation and Optimization Based on Centroidal Voronoi Tessellations. International Journal on Numerical Methods in Engineering, 56(9): 1355-1373.
15. Chen L, Xu J.(2004) Optimal Delaunay Triangulations. Journal of Computational Mathematics, 22(2): 299-308.
16. Chen L.(2004) Mesh Smoothing Schemes Based on Optimal Delaunay Triangulations. In Proceedings of 13th International Meshing Roundtable, 109-120.
17. Zhang Y, Bajaj C, Sohn B S.(2005) 3D Finite Element Meshing from Imaging Data. Computer Methods in Applied Mechanics and Engineering, 194(48-49): 5083-5106.
18. Zhang Y, Bajaj C, Xu G.(2005) Surface Smoothing and Quality Improvement of Quadrilateral/Hexahedral Meshes with Geometric Flow. In 14th International Meshing Roundtable, 449-468.
19. Liu J, Sun S.(2006) Small Polyhedron Reconnection: A New Way to Eliminate Poorly-shaped Tetrahedra. In: Proceedings of the 15th International Meshing Roundtable, 241-257.
20. Xu G.(2008) Geometric Partial Differential Equation Methods in Computational Geometry. Scientific Publishing Press.
21. Ghadyan H R.(2009) Tetrahedral Meshes: Generation, Boundary Recovery and Quality Enhancements.
22. Misztal M K, Brentzen J A, Anton F, Erleben K.(2009) Tetrahedral Mesh Improvement Using Multi-face Retriangulation. In Proceedings of the 18th International Meshing Roundtable, 539-555.
23. Wang J, Yu Z.(2009) A Novel Method for Surface Mesh Smoothing: Applications in Biomedical Modeling. In Proceedings of the 18th International Meshing Roundtable, 195-210.
24. Lederman C, Joshi A, Dinov I, Van Horn J D, Vese L, Toga A.(2010) Tetrahedral Mesh Generation for Medical Images with Multiple Regions using Active Surfaces. 2010 IEEE International Symposium on Biomedical Imaging From Nano to Macro, 436-439.
25. Qian J, Zhang Y, Wang W, Lewis A C, Siddiq Qidwai M A, Geltmacher A B.(2010) Quality Improvement of Non-manifold Hexahedral Meshes for Critical Feature Determination of Microstructure Materials. International Journal for Numerical Methods in Engineering, 82(11): 1406-1423.
26. Zhang Y, Hughes T, Bajaj C.(2010) An Automatic 3D Mesh Generation Method for Domains with Multiple Material. Computer Methods in Applied Mechanics and Engineering, 199(5-8): 405-415.